



Inhibition of VDAC1 Protects Against Glutamate-Induced Oxytosis and Mitochondrial Fragmentation in Hippocampal HT22 Cells

Pandian Nagakannan¹ · Md Imamul Islam¹ · Soheila Karimi-Abdolrezaee¹ · Eftekhar Eftekharpour¹ 

Received: 3 October 2018 / Accepted: 7 November 2018 / Published online: 12 November 2018
© Springer Science+Business Media, LLC, part of Springer Nature 2018

Abstract

The involvement of glutamate in neuronal cell death in neurodegenerative diseases and neurotrauma is mediated through excitotoxicity or oxytosis. The latter process induces oxidative stress via glutamate-mediated inhibition of cysteine transporter xCT, leading to depletion of the cellular glutathione pool. Mitochondrial damage, loss of mitochondrial membrane potential (MMP), and depletion of energy metabolites have been shown in this process. The Voltage-Dependent Anion Channel-1 (VDAC1) is one of the main components of the mitochondrial outer membrane and plays a gatekeeping role in mitochondria-cytoplasm transport of metabolites. In this study, we explored the possible participation of VDAC-1 in the pathophysiology of oxytosis. Administration of glutamate in HT22 cells that lack the glutamate ionotropic receptors induced an upregulation and oligomerization of VDAC1. This was associated with an increase in ROS and loss of cell survival. Glutamate-mediated oxytosis in this model also decreased MMP and promoted ATP depletion, resulting in translocation of cytochrome c (cyt C) and apoptosis inducing factor (AIF) from mitochondria into the cytosol. This was also accompanied by cleavage of AIF to form truncated AIF. Inhibition of VDAC1 oligomerization using 4,4'-Diisothiocyanatostilbene-2,2'-disulfonate (DIDS), significantly improved the cell survival, decreased the ROS levels, improved mitochondrial functions, and decreased the mitochondrial damage. Notably, DIDS also inhibited the mitochondrial fragmentation caused by glutamate, indicating the active role of VDAC1 oligomerization in the process of mitochondrial fragmentation in oxytosis. These results suggest a critical role for VDAC1 in mitochondrial fragmentation and its potential therapeutic value against glutamate-mediated oxidative neurotoxicity.

Keywords Glutamate toxicity · Ferroptosis · Caspase-independent apoptosis · Oxidative stress · AIF · DIDS

Introduction

Glutamate is an important excitatory neurotransmitter in the central nervous system (Fonnum 1984; Zhou and Danbolt 2014). A large volume of literature during the last two decades has identified the importance of glutamate-mediated regulation and release of many active substances from astrocytes; a process known as gliotransmission that can affect neuronal function (Santello et al. 2012; Sahlender et al. 2014; Savtchouk and Volterra 2018). In normal physiological conditions, a sophisticated glutamate uptake system is responsible for maintaining an optimal concentration of

extracellular glutamate. Pathological accumulation of glutamate in neurodegenerative diseases (ND) or after trauma (Lewerenz and Maher 2015) results in excessive neuronal activation and promotion of oxidative damage and neuronal death, a process known as neuronal excitotoxicity, a term coined in 1969 (Olney 1969). This is mediated by activation of ionotropic glutamate receptors, leading to excessive Ca^{2+} influx and induction of apoptosis. A non-apoptotic form of neuronal cell death known as oxytosis (Tan et al. 2001) was identified almost three decades later that is mediated by glutamate-mediated inhibition of glutathione (GSH) synthesis. A cystine/glutamate transporter (xCT antiporter) in neurons is responsible for the uptake of cystine from the extracellular space in exchange for the intracellular glutamate. Cystine is then reduced to cysteine and is used for GSH synthesis. Excessive extracellular glutamate will inhibit the xCT antiporter, leading to GSH deficiency. Oxytosis has been well studied in the HT22 cell line, an

✉ Eftekhar Eftekharpour
eftekh@umanitoba.ca

¹ Department of Physiology and Pathophysiology, Regenerative Medicine Program and Spinal Cord Research Centre, University of Manitoba, Winnipeg, Canada

immortalized model of murine hippocampal neurons that lack ionotropic glutamate receptors and therefore glutamate toxicity is mainly due to xCT blockage. Oxytosis can also be induced by depletion of GSH using buthionine sulfoximine, an inhibitor γ -glutamylcysteine synthetase that is essential for GSH synthesis (Lewerenz et al. 2018).

Ferroptosis is another form of programmed cell death in cancer cells that has recently gained widespread attention (Dixon et al. 2012). This is an iron-dependent mechanism of cell death, which is observed after inhibition of xCT antiporter by erastin and sulfasalazine and is identified by excessive lipid peroxidation due to depleted glutathione peroxidase-4 activity. Oxytosis and ferroptosis share many similarities including mitochondrial dysfunction that is manifested by loss of mitochondrial membrane potential, reduced ATP production, and mitochondrial fragmentation. Additionally, both oxytosis and ferroptosis have been identified to follow a caspase-independent pathway of cell death (Lewerenz et al. 2018).

The voltage-dependent anion channel 1 (VDAC1) is located in the outer mitochondrial membrane (OMM) and is a major regulator of metabolic cross-talk between the mitochondrial compartment and the cytosol. VDAC1 plays a key role in maintaining the mitochondrial physiology through mediating the transport of several metabolites including adenine nucleotides and pyruvate across the OMM and regulation of ionic movement, such as Ca^{2+} , and as well as controlling ROS production (McCommis and Baines 2012; Shoshan-Barmatz and Mizrachi 2012).

The involvement of VDAC1 in the pathophysiology of ND has been suggested because of its upregulation in post-mortem brain samples from patients affected with Alzheimer's disease (AD) and mouse models of AD (Shoshan-Barmatz et al. 2018; Reddy 2013). In addition, VDAC1 has been shown to play a key role in mitochondrial dysfunction in AD (Manczak and Reddy 2012). Recently, inhibition of VDAC1 was shown to prevent mitochondrial fragmentation in a model of cardiac ischemia/reperfusion (Chaanine et al. 2013). Disruption of mitochondrial membrane potential, energy production, and mitochondrial dynamics have been found to precede the onset of ND (Su et al. 2010).

The role of VDAC1 in regulation of mitochondria-dependent apoptosis is well studied; under various types of apoptotic stimuli, VDAC1 was demonstrated to undergo oligomerization and form a transition pore to facilitate OMM permeability, leading to the release of cytochrome C and activation of the caspase cascade (Keinan et al. 2010). However, the involvement of mitochondrial VDAC1 in glutamate/erastin-mediated toxicity has not been adequately examined. In this study, we used the HT22 oxytosis/ferroptosis model and showed that VDAC1 oligomerization is one of the underlying molecular mechanisms involved in this form of cell death. Application of a VDAC1 inhibitor

can successfully abolish its oligomerization and prevent cell death, suggesting that targeting this anion channel could be a potential therapeutic approach for treating disease associated with mitochondrial dysfunction.

Materials and Methods

This study was performed according to the guidelines of the University of Manitoba Biosafety permit (BB0189-2).

Reagents

L-Glutamic acid was purchased from Sigma. Cell Counting Kit-8 (CCK-8, #CK04) was from Dojindo Molecular Technologies, Japan. ATP determination kit (#A22066), Cell-ROX™ Deep Red Reagent (#C10422), and MitoTracker™ Red CMXRos (#M7512) were from Molecular Probes, USA. Halt Protease and phosphatase inhibitor cocktail, Pierce BCA Protein Assay Kit (#23225), and EGS (ethylene glycol bis(succinimidyl succinate)) were from Thermo Scientific, USA. Erastin and DIDS (4,4'-Diisothiocyanatostilbene-2,2'-disulfonate) were from Tocris, Bioscience, UK. TMRM (Tetramethylrhodamine methyl ester, perchlorate, #70017) was from Biotium, Inc., USA. FCCP (Carbonyl cyanide 4-(trifluoromethoxy)phenylhydrazone) was from Cayman, USA.

Cell Culture, Treatments, and Determination of Cell Viability

Immortalized hippocampal neurons, HT22 cells were obtained from Salk Institute, CA, USA. These cells are not listed on the Misidentified Cell Registry (<http://iclac.org/databases/cross-contaminations/>). The cells were cultured in DMEM (Dulbecco's modified Eagle's medium) containing 4.5 g/L glucose supplemented with 2 mM glutamine, 1 mM Sodium Pyruvate, 1% PSN (penicillin, streptomycin and neomycin), and 10% heat inactivated Fetal Bovine Serum at 37 °C in a humidified incubator containing 5% CO_2 .

Cells were seeded at a density of 10,000 cells/well in a 96-well plate and cultured overnight in growth medium prior to the treatments. To determine cell viability, cells were treated with glutamate alone or in combination with DIDS in volume of 100 μl for 12 h, after which 10 μl of Cell Counting Kit-8 (CCK-8) reagent was added to each well and incubated for 4 h at 37 °C. Absorbance at 450 nm with a background correction at 650 nm was measured using Synergy H1 Hybrid Reader (BioTeK Instruments, USA) and the relative cell viability was presented as percentage of control.

Subcellular Fractionation

Cytosolic fractions were prepared using standard Cell Fractionation kit from abcam©, following the manufacturer's protocol. Briefly, the cells were scraped, washed twice with PBS, and suspended in ice-cold fractionation buffer (20 mM HEPES [pH 7.4], 250 mM sucrose, 1.5 mM MgCl₂, 10 mM KCl, 1 mM EGTA, 1 mM EDTA) with protease and phosphatase inhibitors and incubated for 20 min on ice. The cell suspension was passed through a 25 G needle attached to a 1 ml syringe and incubated for an additional 20 min on ice. The lysate was centrifuged at 10,000×g for 10 min at 4 °C to pellet out the nuclei and mitochondria and the supernatant was collected in a fresh Eppendorf tube and was further centrifuged at 21,000×g for 2 h and the supernatant was collected as cytosol.

Western Blot Analysis

Western blotting was performed according to our routine procedures (Nagakannan et al. 2016). Briefly, at the termination of the experiment, cells were scraped, washed with PBS and pelleted by centrifugation, and the pellets were lysed in ice-cold NP-40 lysis buffer (1% NP-40 in buffer containing 50 mM Tris HCl [pH 8], 150 mM NaCl, 5 mM EDTA) with added protease and phosphatase inhibitors. The lysates were sonicated (3×5 s pulses) on ice and were centrifuged at 10,000×g for 15 min at 4 °C and the supernatant was collected. The protein content in cell extracts and cytosolic fractions (described above) was determined with the Pierce BCA Protein Assay Kit using BSA as standard and were diluted with 6× Laemmli sample buffer containing β-mercaptoethanol. For non-reducing SDS-PAGE, samples were diluted in sample buffer without β-mercaptoethanol. Equal amounts of proteins from cell lysates and cytosolic fractions were resolved on a SDS-PAGE and blotted onto PVDF membrane. The membranes were blocked with 5% non-fat milk and incubated with the following primary antibodies: VDAC1 (1:1000, #sc-390996), cytochrome C (1:1000, #sc-13156), and AIF (1:1000, #sc-13116) from Santa Cruz Biotechnologies, USA; Bcl-2 (1:1000, #2870) from Cell Signalling Technologies, USA; Histone H3 (1:5000, #ab1791) from abcam, USA. After overnight incubation at 4 °C with the primary antibodies, the membranes were probed with the appropriate HRP-conjugated secondary antibodies and the immunoreactive bands were detected with Clarity™ and Clarity Max™ Western ECL Blotting Substrates (Bio-Rad Laboratories, USA). To confirm equal loading, the membranes were gently stripped using 0.2N NaOH for 15 min and probed for β-Actin (1:5000, #sc-47778-HRP) and the band densities of target proteins as measured using Image J software (NIH, version 1.51j8) or AlphaEaseFC (version 6.0.0, Alpha Innotech, USA)

were normalized to β-Actin. The values of fold change are expressed as mean ± S.E.M.

Chemical Cross-linking

To detect the oligomeric forms of VDAC1, chemical cross-linking of cells using a membrane permeable cross-linker, EGS (ethylene glycol bis(succinimidyl succinate)), was performed as described previously (Keinan et al. 2010). Briefly, at the end of indicated time periods, cells were harvested by scraping, washed twice with PBS, and incubated with 0.5 mM EGS in PBS, pH 7.4 at 30 °C for 20 min. To quench excess cross-linker, 1.5M Tris HCl, pH 7.8 was added to a final concentration of 20 mM and incubated for 5 min at room temperature and the samples were centrifuged at 10,000×g for 5 min. The pellet was lysed in NP-40 lysis buffer by sonication on ice and the protein content was determined using Pierce BCA Protein Assay. Samples (50 μg) were subjected to SDS-PAGE and western blotting using anti-VDAC1 antibody.

Measurement of Reactive Oxygen Species

Cells were cultured on glass coverslips and were treated with glutamate alone or in combination with DIDS for 8 h. At the end of treatment period, cells were incubated with 2.5 μM CellROX™ Deep Red reagent at 37 °C for 30 min. Then the cells were washed with PBS and fixed with paraformaldehyde (3%) in PBS, stained with DAPI (1: 10,000), and visualized using a LSM710 Zeiss confocal microscope (Zeiss, Germany) at Ex/Em: 633 nm/697 nm. The mean fluorescence intensity emitted from CellROX staining per cell was measured using Image J software.

Mitochondrial Membrane Potential

Cells were cultured on a μ-slide 8-well chamber (Ibidi GmbH, Germany) and were exposed to 2 mM glutamate or 250 μM DIDS alone or in combination for 12 h. Then the cells were washed once with PBS and incubated with 100 nM TMRM (Tetramethylrhodamine methyl ester) in growth medium at 37 °C for 30 min (Voronina et al. 2004). At the end of incubation, medium was replaced with fresh medium and the images were acquired at far length wavelength (Ex/Em: 514 nm/610 nm) using LSM710 Zeiss confocal microscope and the mean fluorescence intensity per cell was quantified by Image J software.

Mitochondrial Morphology

Cells cultured on coverslips were subjected to appropriate treatments for 8 h and were incubated with 200 nm MitoTracker™ Red CMXRos for 15 min at 37 °C, after

which the cells were washed once with PBS and fixed with ice-cold 98% methanol at $-20\text{ }^{\circ}\text{C}$ for 10 min. Images were acquired using an LSM710 Zeiss confocal microscope and the brightness and contrast were adjusted using Image J software. An observer blind to the treatment conditions scored the mitochondrial morphology visually as previously described (Rambold et al. 2011). Cells containing elongated and highly interconnected mitochondria were categorized as “tubular,” while cells that had small and spherical mitochondria were scored as “fragmented.” Cells with a mixed population of spherical and shorter tubulated mitochondria were categorized as “intermediate.” At least 350 cells per condition from three independent studies were scored and the percentage of each category were calculated and presented as mean \pm S.E.M.

Determination of ATP Content

Cells were subjected to indicated treatment conditions for 12 h and were harvested, washed twice in PBS, and lysed in 0.1% NP-40 lysis buffer and the ATP content was determined using a commercially available ATP determination kit following the manufacturers’ protocol.

Statistical Analysis

Data are expressed as mean \pm S.E.M. Statistical differences between the treatments were evaluated by one-way analysis of variance (ANOVA) followed by Tukey’s post hoc test using GraphPad Prism Software (version 6.07, California, USA). *p* values less than 0.05 were considered as statistically significant.

Results

Glutamate and Erastin Toxicity Result in Upregulation of VDAC1

Glutamate-induced oxytosis shares many similarities with the recently identified ferroptotic cell death; both these mechanisms of cell death involve GSH depletion through inhibition of xCT antiporter (Lewerenz et al. 2018). To seek the role of VDAC1 in oxytosis/ferroptosis, we used glutamate and erastin as inducers of this novel type of cell death mechanism. A dose–response study was performed to determine the effective concentration of glutamate and erastin for induction of 70–80% cell death in HT22 cells. Cell viability was measured using CCK-8 (water-soluble tetrazolium salt-8) after 12-h administration of glutamate and erastin. A dose of 4 mM glutamate or 500 nM erastin was chosen for these studies (Fig. 1a, b). This is in

agreement with previous reports for this model (Kang et al. 2014; Neitemeier et al. 2017).

To determine the status of VDAC1 in oxytosis, HT22 cells were treated with glutamate or erastin for increasing time durations (8, 12, and 16 h) and the protein expression levels of VDAC1 were assessed by western blotting. Using our routine reducing SDS-PAGE western blotting, a time-dependent increase in the expression of VDAC1 protein levels was observed (Fig. 1c–f). Interestingly, under non-reducing conditions, the intensity of the 35 kDa VDAC1 band (known as VDAC1 monomer) was not notably increased; however, a second band was detected using anti-VDAC1 antibody, which was more pronounced with increasing exposure time of the cells to glutamate and erastin (Fig. 1c, d). Using cross-linking agents like BMOE (bis(maleimido)ethane) or EGS (ethylene glycol bis(succinimidyl succinate)), earlier studies have shown the appearance of this faster migrating monomeric form of the VDAC1 band upon induction of an apoptotic stimuli (Keinan et al. 2013). This band is proposed to be the result of an intra-molecular bond formation between a single cysteine in the N-terminal region and another amino group, possibly a lysine residue (Geula et al. 2012). However, in this experiment shown in Fig. 1c and d, no such cross-linkers were utilized. Cysteine groups in VDACs have been shown to be the target for oxidation by ROS and therefore it is possible that the faster migrating anti-VDAC1 antibody reactive band is a result of intra-molecular disulfide bond formation, although the contribution of this intra-molecular disulfide bond in either pore-conductance or apoptotic induction remains unclear (De Pinto et al. 2016).

Glutamate and Erastin Induce Oligomerization of VDAC1 in HT22 Cells

To seek further insights into the effect of oxidative stress induced by glutamate and erastin on oligomeric status of VDAC1, we performed cross-linking experiments using EGS to capture the oligomeric states of VDAC1 by western blotting. As shown in Fig. 2a, glutamate induced a time-dependent induction in VDAC1 oligomerization evident by the higher molecular weight bands corresponding to the dimeric, trimeric, and multimeric states of VDAC1. Similar results were obtained with erastin treatment (Fig. 2b). The intra-molecular cross-linked monomeric VDAC1 band (indicated by asterisk) with altered electrophoretic migration was also detected in glutamate-treated and erastin-treated HT22 cells (Fig. 2a, b). These results prompted us to examine the possible involvement of VDAC1 oligomerization in cell death after xCT inhibition by glutamate and erastin.

Fig. 1 VDAC1 is upregulated under oxytosis. HT22 cells were treated with increasing concentrations of **a** glutamate or **b** erastin for 12 h and the cell survival was assessed using a CCK-8 assay kit. Values are expressed as mean \pm S.E.M. of averages from $N=4$ (glutamate) and $N=3$ (erastin) independent experiments. HT22 cells were incubated with **c** 4 mM glutamate or **d** 500 nM erastin for the indicated time periods and the cell lysates were subjected to SDS-PAGE under reducing and non-reducing conditions and assessed for the expression of VDAC1 protein. Representative western blots are shown in **c** and **d** with corresponding densitometric analysis of VDAC1 (in reducing SDS-PAGE) normalized to β -actin shown in **e** and **f**. Values are expressed as mean \pm S.E.M. of averages from $N=3$ independent experiments, * $p < 0.05$, ** $p < 0.01$, and **** $p < 0.0001$. Arrows indicate the faster migrating monomeric form of VDAC1 band with possible oxidative modification

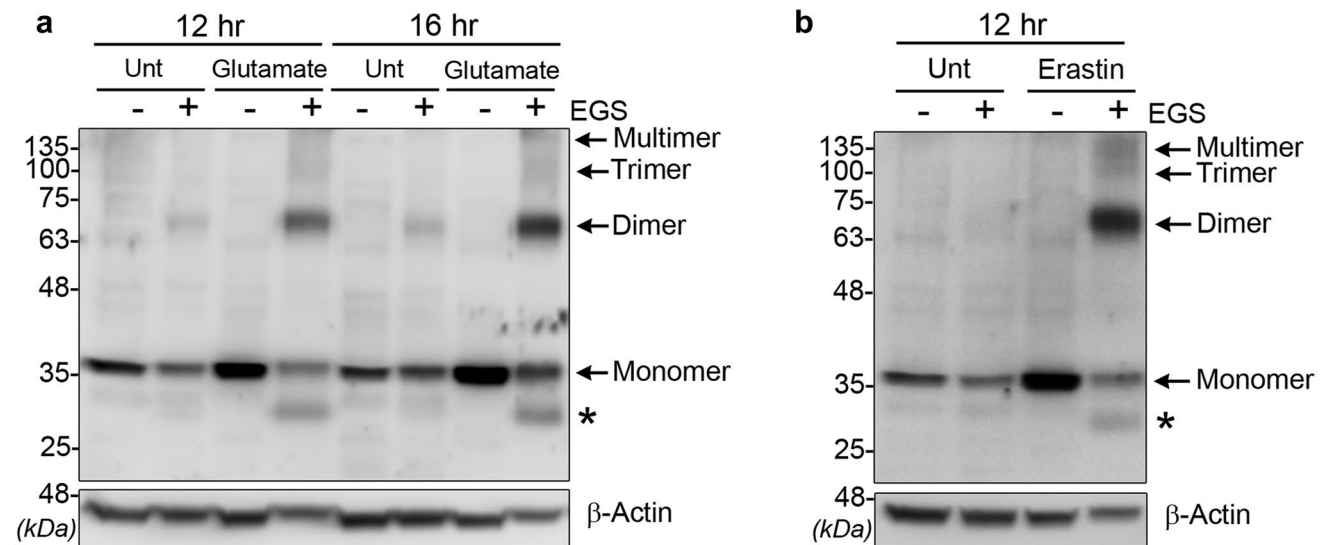
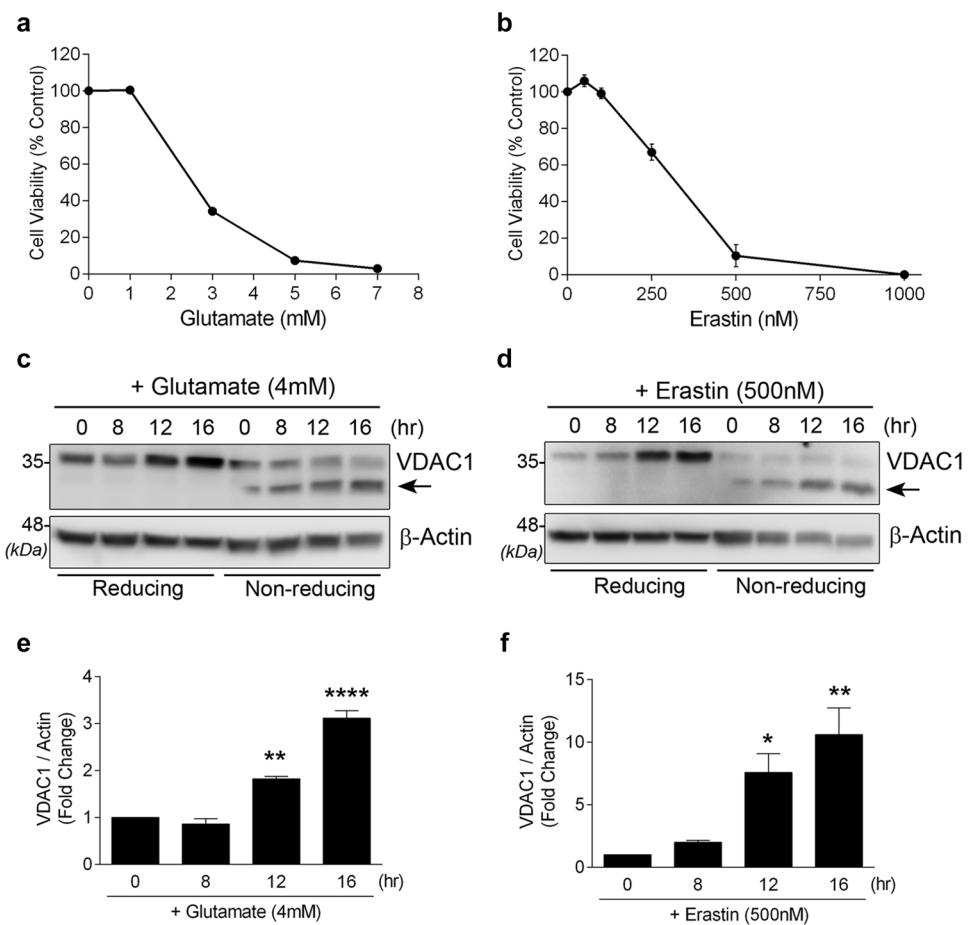


Fig. 2 Glutamate and erastin induce VDAC1 oligomerization. HT22 cells were treated with **a** 4 mM glutamate or **b** 500 nM erastin for indicated time periods and the cells were harvested and incubated at 30 °C for 20 min in the presence or absence of EGS to cross-link the proteins and subjected to western blotting to assess the oligomeric

status of VDAC1. Note the multifold increase in dimer, trimer, and multimeric forms of VDAC1 in glutamate-treated and erastin-treated samples from untreated cells. Asterisk indicates the intra-molecular cross-linked bands. Representative blots are shown here; similar results were observed in two independent experiment

Inhibition of VDAC1 Oligomerization by DIDS Prevents Glutamate- and Erastin-Induced Cell Death

To test the hypothesis that inhibition of VDAC1 might protect against glutamate- or erastin-induced cell death, we used DIDS, a VDAC1 inhibitor (Ben-Hail and Shoshan-Barmatz 2016). HT22 cells were treated with glutamate or erastin in the absence or presence of increasing concentrations (50–300 μM) of DIDS for 12 h and the cell survival was assessed by CCK-8 assay. A dose-dependent improvement in cell survival was observed with DIDS treatment in the presence of glutamate and erastin, indicating the potential involvement of VDAC1 in the mediation of cell death after xCT inhibition (Fig. 3a). Inhibition of VDAC1 has been shown to be detrimental under normal conditions as VDAC1 is involved in several cellular homeostatic functions such as transport of ions and ATP (Pamenter et al. 2013; Shoshan-Barmatz and Mizrachi 2012). In agreement with previous reports, at a concentration of 300 μM , DIDS alone showed a significant decrease in cell survival under normal conditions. Hence, we used a concentration of 250 μM DIDS as the effective dose for this study; the efficacy of the selected dose of DIDS was confirmed by a VDAC1 cross-linking assay. As shown in Fig. 3c, DIDS effectively abrogated the induction of VDAC1 oligomerization as evident by the absence of the trimeric and multimeric higher molecular weight bands and a significant decrease in dimeric and intra-molecular cross-linked bands in cells treated with glutamate-DIDS combination. Interestingly, DIDS also inhibited the upregulation of VDAC1 caused by glutamate (Fig. 3d).

Inhibition of VDAC1 Abrogates ROS Generation and Promotes Mitochondrial Integrity

Mitochondria are the major source of ROS and VDAC1 has been shown to participate in ROS release from mitochondria to cytosol (DeHart et al. 2018). To investigate the involvement of VDAC1 in generation of ROS in oxytosis, cells were treated with glutamate in the absence or presence of DIDS for 8 h and the accumulation of ROS was assessed by a cell permeable probe, CellROX[®]-far red reagent. This probe is oxidized by soluble ROS and produces a strong fluorescent signal. Glutamate-treated cells showed a 2.54 fold increase in ROS levels in comparison to untreated control cells. Administration of DIDS effectively decreased the ROS levels to near normal (Fig. 4a, b). To examine the mechanism of VDAC1 involvement in oxytosis-induced mitochondrial damage, we first tested the levels of pro-survival protein Bcl2 in whole cell lysates. Glutamate caused a significant reduction of Bcl-2 protein by 47%, which was markedly prevented by DIDS (Fig. 4c and d). This was associated with increased mitochondrial membrane integrity as confirmed by subcellular fractionation. Administration of

4 mM glutamate to HT22 cells caused a robust increase in cytosolic level of total AIF and cyt C, indicating mitochondrial membrane damage. Treatment with a VDAC1 inhibitor, DIDS, significantly decreased the amount of total AIF and cyto C in the cytosol, indicating preserved mitochondrial integrity (Fig. 4e, f). Previous studies have identified that in caspase-independent apoptotic insults, AIF is cleaved to form a 57 kDa truncated form that is translocated from mitochondria to the cytosol and the nucleus, where it causes DNA fragmentation (Otera et al. 2005). This AIF cleavage is mediated by Calpains that are activated by Ca^{2+} overload (Polster et al. 2005; Lewerenz et al. 2018). In line with these earlier reports, we observed that glutamate treatment enhances the levels of AIF full length and cleaved forms in the cytosolic fraction; this was significantly reduced by DIDS treatment (Fig. 4e). Interestingly, we observed that Histone H3, a core component of chromatin, is affected by glutamate-mediated oxytosis. A cleaved product of Histone H3 with a molecular weight of around 10 kDa was detectable only in cells exposed to glutamate and was completely abolished with DIDS treatment (Fig. 4e).

VDAC1 Mediates Mitochondrial Dysfunction in Oxytosis

Mitochondrial fragmentation is a hallmark of xCT inhibition-induced oxytosis. To elucidate the participation of VDAC1 in mitochondrial fragmentation, MitoTracker staining was used after treatment of cultures with 4 mM glutamate alone or in combination with 250 μM DIDS for 8 h. Un-biased analysis of fluorescent images by an observer blinded to the experimental conditions showed that in untreated control cells, $91.0 \pm 2.9\%$ of cells displayed tubular/elongated mitochondria, while only $2.4 \pm 1.5\%$ contained fragmented mitochondria. In marked contrast to the controls, exposure to glutamate resulted in mitochondrial fragmentation in $89.9 \pm 4.5\%$ of cells, while only $4.2 \pm 3.1\%$ cells exhibited tubular mitochondria. The remainder of the cells (around 6%) showed intermediate morphology in both untreated and glutamate-treated cells (Fig. 5a, b). Inhibiting VDAC1 channel with DIDS significantly decreased the percentage of fragmented mitochondria to $27.1 \pm 12.8\%$ and increased the tubular phenotype to $48.3 \pm 15.3\%$ in glutamate-treated cells, while the remaining cells were all found to be in the intermediate category ($24.6 \pm 3.6\%$) (Fig. 5a, b). Mitochondrial fragmentation in response to increased oxidative stress has been associated with defects in mitochondrial respiration, ATP production, membrane depolarization, and ultimately cell death (Knott et al. 2008). We therefore examined the effect of these treatments on cellular ATP. A significant depletion of ATP in glutamate-treated cells was observed, although this was effectively abrogated by inhibition of VDAC1 with DIDS treatment (Fig. 5c).

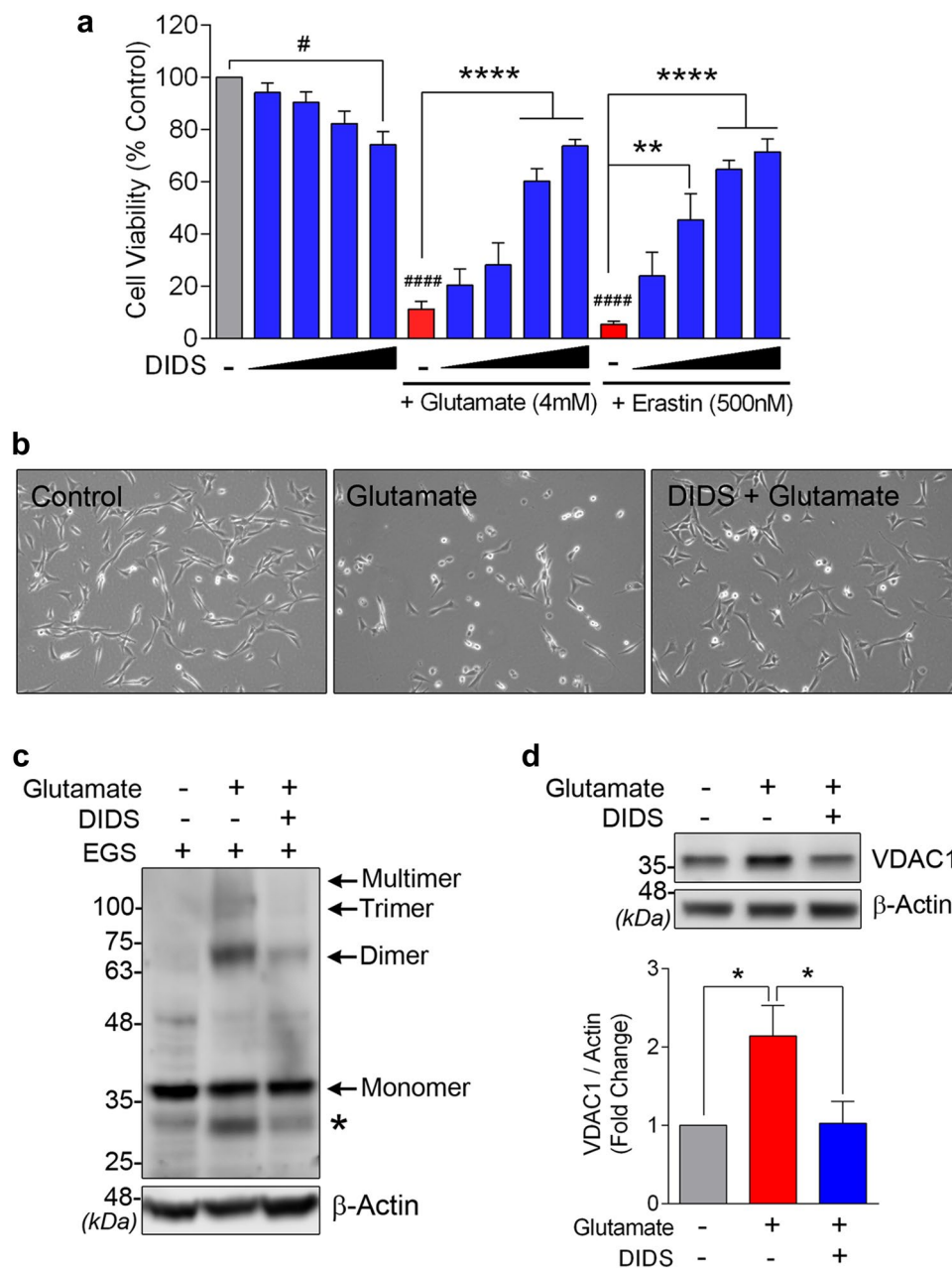


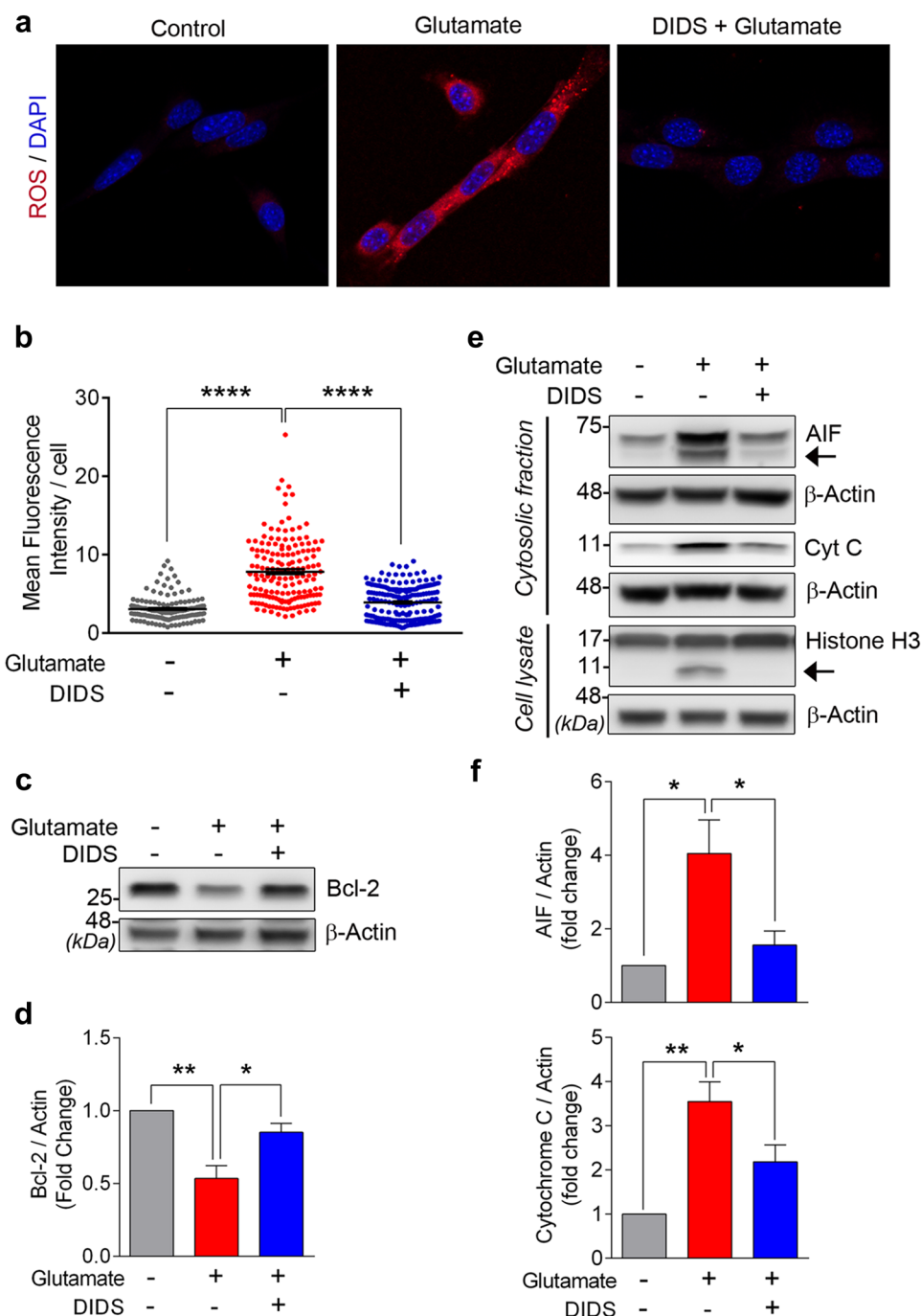
Fig. 3 Inhibition of VDAC1 abrogates glutamate-induced cell death in HT22 cells. **a** HT22 cells were treated with either glutamate (4 mM) or erastin (500 nM) in the presence or absence of increasing concentrations of DIDS (50, 100, 200, and 300 μM, indicated by black triangle) for 12 h and cell survival was assessed using a CCK-8 assay kit. Values are expressed as mean ± S.E.M. of averages from $N=3-4$ independent experiments, # $p < 0.01$ and #### $p < 0.0001$ versus untreated control; ** $p < 0.01$ and **** $p < 0.0001$ versus glutamate or erastin alone. **b** Bright-field images showing the morphological changes (cell shrinkage) and cell loss induced by glutamate (for 12 h) in HT22 cells; addition of DIDS (250 μM) markedly ameliorated

the effects of glutamate and preserved the normal morphology of cells. HT22 cells were treated with glutamate alone or in combination with DIDS (250 μM) for 12 h and the cells were processed for chemical cross-linking with EGS (**c**) or regular western blotting (**d**). DIDS treatment prominently decreased the (**c**) levels of VDAC1 oligomers and intra-molecular cross-linked band (indicated by asterisk) and (**d**) VDAC1 protein expression induced by glutamate. Representative blots are shown here and the quantification of VDAC1 protein normalized to β-actin is presented as bar graph and the values are expressed as mean ± S.E.M. of averages from $N=4$ independent experiments, * $p < 0.05$

The mitochondrial response to glutamate was further tested by assessment of mitochondrial membrane potential (MMP) using TMRM. The glutamate concentration used for

these experiments was 2 mM, as 4 mM treatment resulted in significant cell death, making it impossible to generate usable fluorescent images for quantification. Cells were

Fig. 4 Inhibition of VDAC1 mitigates the accumulation of ROS and mitochondrial permeability in HT22 cells exposed to glutamate. **a** HT22 cells were treated with glutamate (4 mM) alone or in combination with DIDS (250 μ M) for 8 h and stained with CellROX deep red reagent (red) and counterstained with DAPI to identify the nucleus (blue). Representative images are shown here. The mean fluorescence intensity per cell was quantified in $n \geq 140$ cells/condition and the distribution of values is presented as dot plot (**b**); lines indicate mean \pm S.E.M. **** $p < 0.0001$; similar results were obtained from two independent experiments. **c** Representative western blot of Bcl-2 in lysates obtained from HT22 cells incubated with glutamate (4 mM) in the absence or presence of DIDS (250 μ M) for 12 h and (**d**) the quantification is shown. Values are expressed as mean \pm S.E.M. of averages from $N = 3$ independent experiments, * $p < 0.05$ and ** $p < 0.01$. **e** HT22 cells were treated with glutamate alone or in combination with DIDS for 12 h and the cytosolic fractions were isolated and assessed for AIF and cytochrome c (Cyt C) by western blotting. The densitometric measurements of AIF and cyt c normalized to β -actin are shown in (**f**) and the values represent mean \pm S.E.M. of averages from $N = 4$ independent experiments, * $p < 0.05$ and ** $p < 0.01$. In a separate set of experiments with similar treatment conditions, lysates were assessed for Histone H3 by western blotting (**e**). Arrows indicate the cleaved bands



subjected to treatments for 12 h and stained with TMRM for immediate live imaging. A significant reduction in averaged cellular TMRM fluorescence intensity was observed in glutamate-treated cells, indicative of a reduced MMP; however, TMRM fluorescence was significantly increased after treatment with DIDS. To test whether inhibition of VDAC1 is sufficient to increase the cellular MMP, control HT22 cells were treated with 250 μ M of DIDS alone, which showed a similar increase in TMRM fluorescence (Fig. 6). Mitochondrial uncoupler FCCP was used as a positive control for

reduction of MMP, which showed a rapid decrease in MMP within 15 min of treatment (Fig. 6).

Discussion

Depletion of GSH due to inhibition of xCT by glutamate/erastin triggers an exponential accumulation of intracellular ROS and a concomitant increase in Ca^{2+} influx through either cGMP-dependent processes or activation of 12/15

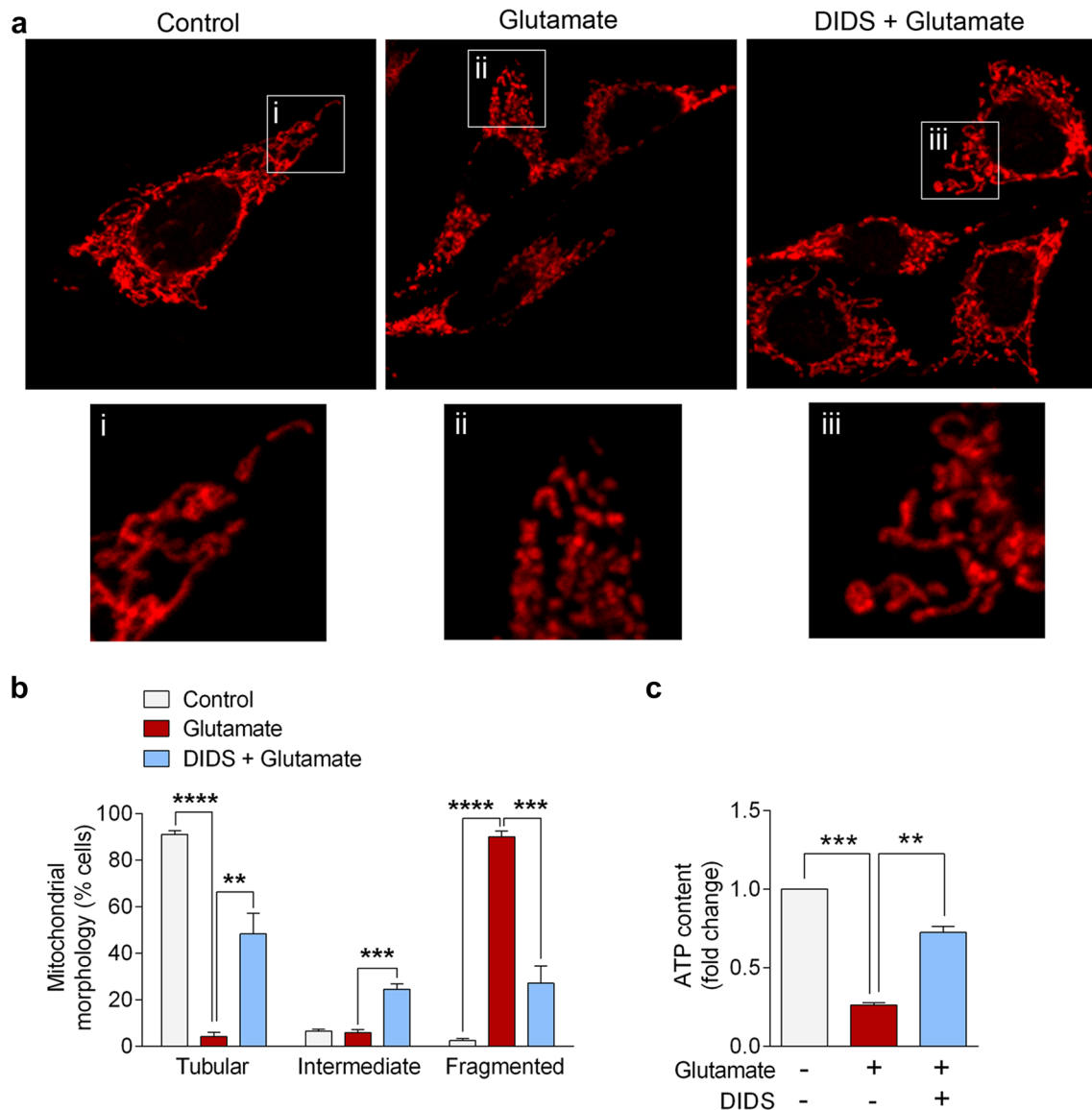


Fig. 5 VDAC1 mediates glutamate-induced mitochondrial fragmentation in HT22 cells. **a** HT22 cells were incubated with 4 mM glutamate in the absence or presence of DIDS (250 μ M) for 8 h and stained with MitoTracker Red CMXRos reagent and the images were acquired using confocal microscopy. Representative images showing the mitochondrial morphology with different treatment conditions are shown. The magnified view of the boxed areas is shown in the bottom row. **b** The mitochondrial morphology was scored by visual inspection by an observer blinded to experimental conditions and the cells were categorized into three subtypes based on the mitochondrial

phenotype exhibited: elongated and highly interconnected (tubular); small and spherical (fragmented); mixed population of spherical and shorter tubulated (intermediate). Values represent mean \pm S.E.M. of percentages from $N=3$ independent experiments, ** $p < 0.01$, *** $p < 0.001$, and **** $p < 0.0001$. **c** ATP content in cell extracts obtained from HT22 cells treated with glutamate (4 mM) or glutamate + DIDS (250 μ M) for 12 h were measured and the values are expressed as mean \pm S.E.M. of averages from two independent experiments, ** $p < 0.01$ and **** $p < 0.0001$

lipoygenase pathway. The Ca^{2+} conducting channels such as ORAI1 and TRPC1 channels have been shown to be involved in this process (Maher et al. 2018). VDAC1 maintains the mitochondrial Ca^{2+} homeostasis by acting as a Ca^{2+} channel. Oligomerization of VDAC1 has been reported in conditions associated with elevated ROS and Ca^{2+} levels. This has been substantiated by targeting VDAC1, using its

inhibitor ruthenium red, which was found to decrease ROS levels and mitochondrial Ca^{2+} uptake and hence attenuate apoptosis (Keinan et al. 2013). In the present study, glutamate treatment caused a significant increase in ROS and diminished MMP and ATP production, signifying mitochondrial dysfunction. Being located in the OMM, VDAC1 plays a gatekeeping role in mitochondria-cytoplasm transport of

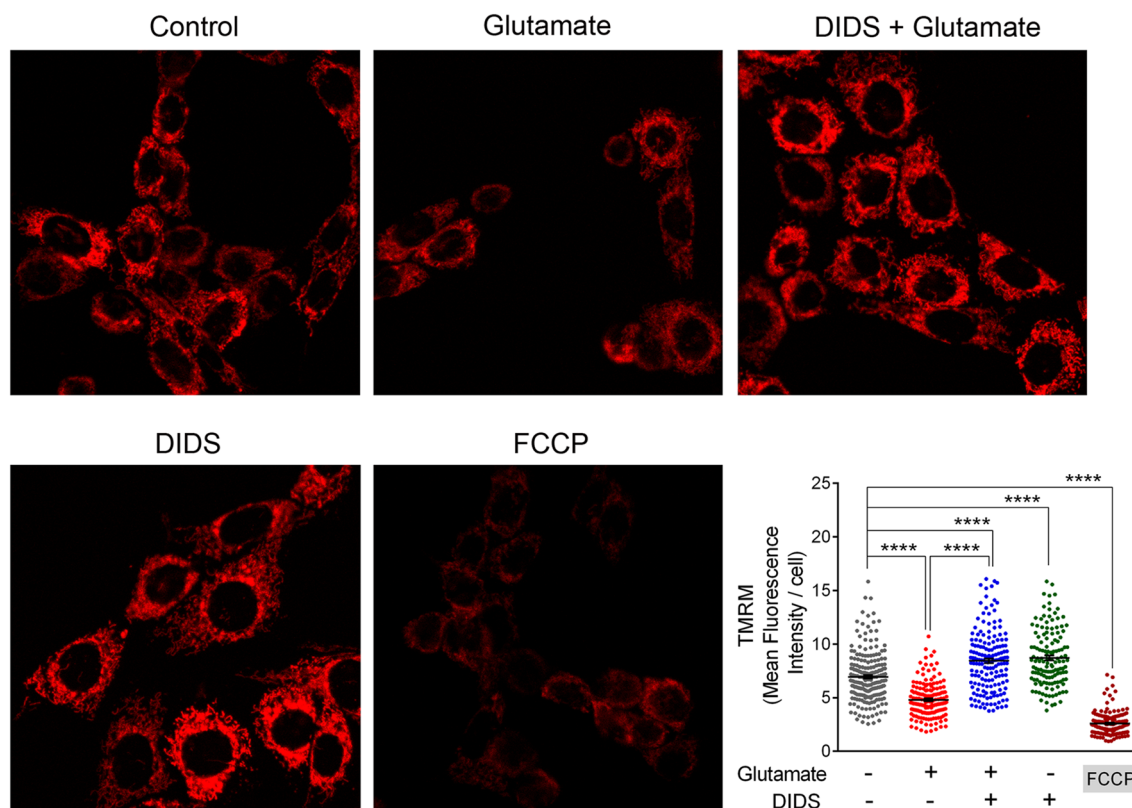


Fig. 6 Inhibition of VDAC1 prevents glutamate-induced disruption of mitochondrial membrane potential. HT22 cells were treated with 2 mM glutamate alone or in combination with DIDS (250 μ M) for 12 h and were stained with TMRM and live-cell images were acquired using confocal microscopy. To avoid any interference of DIDS on TMRM fluorescence, the images were acquired at far length

wavelength (610 nm). Cells treated with FCCP for 15 min were used as positive control. The mean fluorescence intensity per cell was quantified in $n \geq 135$ cells/condition and the dot plot represents the distribution of values; lines indicate mean \pm S.E.M. **** $p < 0.0001$. Similar results were obtained from two independent experiments

mitochondrial metabolites, nucleotides, and ions, and therefore inhibition of VDAC1 with DIDS significantly decreased the ROS levels and improved the mitochondrial functions as evidenced by the increase in MMP and ATP levels. These results suggest the potential involvement of VDAC1 oligomerization in the mediation of mitochondrial damage under oxidative stress. The significant increase in MMP after DIDS treatment in normal cells may reflect the importance of Ca^{2+} levels in mitochondrial membrane polarization. Our results suggest that VDAC1 could possibly be one of the major channels for Ca^{2+} uptake in normal conditions, and hence its inhibition leads to membrane hyperpolarization (Shoshan-Barmatz et al. 2017).

VDAC1 has been shown to be regulated by various Bcl-2 family proteins and Hexokinases (Shoshan-Barmatz et al. 2009). Anti-apoptotic proteins like Bcl-2, Bcl-x1, and HK have been shown to bind the N-terminal region of VDAC1 and inhibit mitochondria-mediated apoptosis (Abu-Hamad et al. 2009), while the interaction with pro-apoptotic Bcl-2 members such as Bax and Bim promotes apoptosis (Liu et al. 2015). This physical interaction leads

to stabilization of oligomeric forms of VDAC1 (Malia and Wagner 2007). Oligomerization of VDAC1, either homodimeric or heterodimeric, causes the mitochondrial pore formation that allows the release of mitochondrial contents into the cytosol, which eventually leads to cell death (McCommis and Baines 2012). In our study, glutamate treatment was associated with a significant reduction in the levels of Bcl-2 protein, suggesting a key role for Bcl-2 in regulation of VDAC1 oligomerization in oxytosis. This is in agreement with previous reports showing the involvement of Bcl-2 in inhibition of VDAC1 oligomerization (Malia and Wagner 2007). The ubiquitin proteasome system (UPS) has also been shown to participate in glutamate-mediated oxytosis in HT22 cells, where inhibition of UPS protected against glutamate cytotoxicity (van Leyen et al. 2005), indicating excessive degradation of vital pro-survival proteins including Bcl2 (Edison et al. 2017). Inhibition of VDAC1 in this study was associated with preserved levels of Bcl-2 levels, although whether UPS activation is the cause or consequence of VDAC1 activation remains to be examined.

Oligomerization of VDAC1 leads to the formation of transition pores in the OMM leading to the translocation of pro-apoptotic proteins such as cyt C and AIF from mitochondria to cytosol (Shoshan-Barmatz et al. 2010). Although, cyt C and AIF release is a classical factor in activation of caspases during apoptosis, the glutamate-mediated oxytosis in HT22 cells is known to occur independent of caspase activation. The major distinguishing feature of oxytosis from caspase-dependent apoptosis is the lack of ATP, which is essential for the assembly of apoptosome and consequent activation of caspases (Fukui et al. 2009). Here, the AIF released from the mitochondria in oxytosis translocates to the nucleus to cause DNA fragmentation, which is an ATP-independent process (Daugas et al. 2000; Fukui et al. 2009). This step is considered to be the final executioner phase in oxytosis. Treatment with DIDS showed a distinct decrease in cytosolic levels of cyt C and AIF, affirming the formation of VDAC1 oligomeric transition pore and its pivotal role in release of these pro-apoptotic mediators. Additionally, the level of truncated AIF was markedly decreased in DIDS-treated cells exposed to glutamate, indicating lesser activation of calpain. Furthermore, the cleavage of Histone-H3 confirms the nuclear damage caused by glutamate, which was prevented by DIDS treatment. Histone molecules have been identified as substrates for several proteases, however, the specific mechanism of Histone H3 degradation in glutamate-mediated oxytosis remains to be explored.

The mitochondrion is a highly dynamic network of organelles that constantly undergo changes in their morphology through fusion and fission processes. Any abnormalities in these dynamics are often associated with impaired mitochondrial functions, energy generation, and integrity and eventually neuronal cell death as seen in several ND (Itoh et al. 2013). Several members of the GTPase family are involved in maintaining the balance between the mitochondrial fission and fusion. Dynamin-related protein-1 (Drp1) and fission 1 (Fis1) are the key players in inducing mitochondrial fission, while Mitofusins (mfn1 and mfn2) and Opa1 serve in maintaining the elongated morphology of mitochondria (Mishra and Chan 2016). Several factors including oxidative stress and ATP depletion are known to disrupt this balance and cause mitochondrial fragmentation (Twig and Shirihai 2011). Considering the fact that VDAC1 is a major player in mediating oxidative stress induced mitochondrial dysfunction, we asked whether inhibition of VDAC1 oligomerization can prevent changes in mitochondrial morphology that is caused by glutamate toxicity. A growing number of studies have shown that glutamate caused a severe decrease in the proportion of elongated to fragmented mitochondria (Landshamer et al. 2008; Sanderson et al. 2015). DIDS treatment effectively prevented this effect suggesting that VDAC1 oligomerization plays an important role in mediating mitochondrial fragmentation.

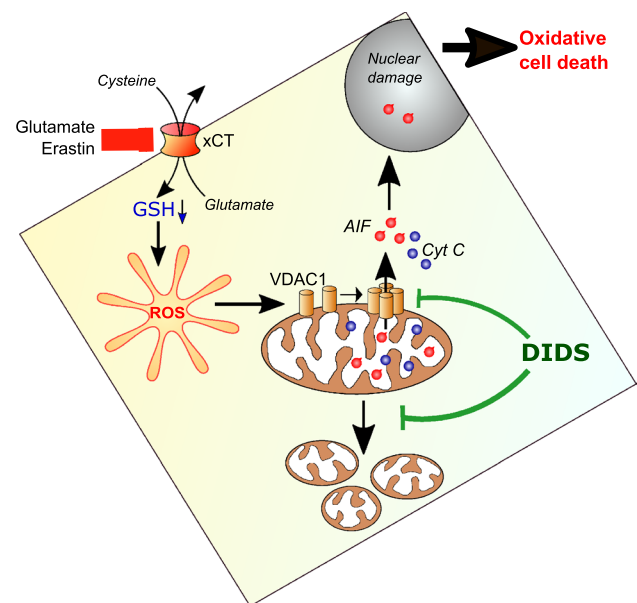


Fig. 7 Excess of glutamate causes a caspase-independent cell death known as “Oxytosis,” by blocking glutathione synthesis. Here, we show that voltage-dependent anion channel-1 (VDAC1) plays a key role in mediation of oxytosis in HT22 cells through formation of a mitochondrial transition pore, thereby facilitating the release of apoptotic inducing factor (AIF) and cytochrome C (Cyt C). Mitochondrial fragmentation is a hallmark of xCT inhibition-induced oxytosis. Blocking VDAC1 oligomerization using DIDS mitigated mitochondrial fragmentation and glutamate-induced oxidative toxicity

The contribution of VDAC1 in glutamate-induced oxytosis/ferroptosis has been summarized schematically in Fig. 7.

In conclusion, we have shown that VDAC1 oligomerization leading to mitochondria-mediated cell death is a shared molecular event between oxytosis and ferroptosis and inhibition of VDAC1 can prevent mitochondrial deficiency and mitigate oxidative neurotoxicity.

Funding Funding was provided by Health Sciences Centre Foundation and Paralyzed Veterans of America.

References

- Abu-Hamad S, Arbel N, Calo D, Arzoino L, Israelson A, Keinan N, Ben-Romano R, Friedman O, Shoshan-Barmatz V (2009) The VDAC1 N-terminus is essential both for apoptosis and the protective effect of anti-apoptotic proteins. *J Cell Sci* 122(Pt 11):1906–1916. <https://doi.org/10.1242/jcs.040188>
- Ben-Hail D, Shoshan-Barmatz V (2016) VDAC1-interacting anion transport inhibitors inhibit VDAC1 oligomerization and apoptosis. *Biochim Biophys Acta* 1863 (7 Pt A):1612–1623. <https://doi.org/10.1016/j.bbamer.2016.04.002>
- Chaanine AH, Gordon RE, Kohlbrenner E, Benard L, Jeong D, Hajar RJ (2013) Potential role of BNIP3 in cardiac remodeling, myocardial stiffness, and endoplasmic reticulum: mitochondrial calcium homeostasis in diastolic and systolic heart failure. *Circ*

- Heart Fail 6(3):572–583. <https://doi.org/10.1161/CIRCHEARTFAILURE.112.000200>
- Daugas E, Susin SA, Zamzami N, Ferri KF, Irinopoulou T, Larochette N, Prevost MC, Leber B, Andrews D, Penninger J, Kroemer G (2000) Mitochondrio-nuclear translocation of AIF in apoptosis and necrosis. *FASEB J* 14(5):729–739
- De Pinto V, Reina S, Gupta A, Messina A, Mahalakshmi R (2016) Role of cysteines in mammalian VDAC isoforms' function. *Biochim Biophys Acta* 1857(8):1219–1227. <https://doi.org/10.1016/j.bbabo.2016.02.020>
- DeHart DN, Fang D, Heslop K, Li L, Lemasters JJ, Maldonado EN (2018) Opening of voltage dependent anion channels promotes reactive oxygen species generation, mitochondrial dysfunction and cell death in cancer cells. *Biochem Pharmacol* 148:155–162. <https://doi.org/10.1016/j.bcp.2017.12.022>
- Dixon SJ, Lemberg KM, Lamprecht MR, Skouta R, Zaitsev EM, Gleason CE, Patel DN, Bauer AJ, Cantley AM, Yang WS, Morrison B, Stockwell BR (2012) Ferroptosis: an iron-dependent form of nonapoptotic cell death. *Cell* 149(5):1060–1072. <https://doi.org/10.1016/j.cell.2012.03.042>
- Edison N, Curtz Y, Paland N, Mamriev D, Chorubczyk N, Haviv-Reingewertz T, Kfir N, Morgenstern D, Kupervaser M, Kagan J, Kim HT, Larisch S (2017) Degradation of Bcl-2 by XIAP and ARTS promotes apoptosis. *Cell Rep* 21(2):442–454. <https://doi.org/10.1016/j.celrep.2017.09.052>
- Fonnum F (1984) Glutamate: a neurotransmitter in mammalian brain. *J Neurochem* 42(1):1–11
- Fukui M, Song JH, Choi J, Choi HJ, Zhu BT (2009) Mechanism of glutamate-induced neurotoxicity in HT22 mouse hippocampal cells. *Eur J Pharmacol* 617(1–3):1–11. <https://doi.org/10.1016/j.ejphar.2009.06.059>
- Geula S, Ben-Hail D, Shoshan-Barmatz V (2012) Structure-based analysis of VDAC1: N-terminus location, translocation, channel gating and association with anti-apoptotic proteins. *Biochem J* 444(3):475–485. <https://doi.org/10.1042/BJ20112079>
- Itoh K, Nakamura K, Iijima M, Sesaki H (2013) Mitochondrial dynamics in neurodegeneration. *Trends Cell Biol* 23(2):64–71. <https://doi.org/10.1016/j.tcb.2012.10.006>
- Kang Y, Tiziani S, Park G, Kaul M, Paternostro G (2014) Cellular protection using Flt3 and PI3Kalpha inhibitors demonstrates multiple mechanisms of oxidative glutamate toxicity. *Nat Commun* 5:3672. <https://doi.org/10.1038/ncomms4672>
- Keinan N, Tyomkin D, Shoshan-Barmatz V (2010) Oligomerization of the mitochondrial protein voltage-dependent anion channel is coupled to the induction of apoptosis. *Mol Cell Biol* 30(24):5698–5709. <https://doi.org/10.1128/MCB.00165-10>
- Keinan N, Pahima H, Ben-Hail D, Shoshan-Barmatz V (2013) The role of calcium in VDAC1 oligomerization and mitochondria-mediated apoptosis. *Biochim Biophys Acta* 1833(7):1745–1754. <https://doi.org/10.1016/j.bbamcr.2013.03.017>
- Knott AB, Perkins G, Schwarzenbacher R, Bossy-Wetzel E (2008) Mitochondrial fragmentation in neurodegeneration. *Nat Rev Neurosci* 9(7):505–518. <https://doi.org/10.1038/nrn2417>
- Landshamer S, Hoehn M, Barth N, Duvezin-Caubet S, Schwake G, Tobaben S, Kazhdan I, Becattini B, Zahler S, Vollmar A, Pellicchia M, Reichert A, Plesnila N, Wagner E, Culmsee C (2008) Bid-induced release of AIF from mitochondria causes immediate neuronal cell death. *Cell death differentiation* 15(10):1553–1563. <https://doi.org/10.1038/cdd.2008.78>
- Lewerenz J, Maher P (2015) Chronic glutamate toxicity in neurodegenerative diseases-what is the evidence? *Front Neurosci* 9:469. <https://doi.org/10.3389/fnins.2015.00469>
- Lewerenz J, Ates G, Methner A, Conrad M, Maher P (2018) Oxytosis/ferroptosis-(Re-) emerging roles for oxidative stress-dependent non-apoptotic cell death in diseases of the central nervous system. *Front Neurosci* 12:214. <https://doi.org/10.3389/fnins.2018.00214>
- Liu Z, Luo Q, Guo C (2015) Bim and VDAC1 are hierarchically essential for mitochondrial ATF2 mediated cell death. *Cancer Cell Int* 15:34. <https://doi.org/10.1186/s12935-015-0188-y>
- Maher P, van Leyen K, Dey PN, Honrath B, Dolga A, Methner A (2018) The role of Ca(2+) in cell death caused by oxidative glutamate toxicity and ferroptosis. *Cell Calcium* 70:47–55. <https://doi.org/10.1016/j.ceca.2017.05.007>
- Malia TJ, Wagner G (2007) NMR structural investigation of the mitochondrial outer membrane protein VDAC and its interaction with antiapoptotic Bcl-xL. *Biochemistry* 46(2):514–525. <https://doi.org/10.1021/bi061577h>
- Manczak M, Reddy PH (2012) Abnormal interaction of VDAC1 with amyloid beta and phosphorylated tau causes mitochondrial dysfunction in Alzheimer's disease. *Hum Mol Genet* 21(23):5131–5146. <https://doi.org/10.1093/hmg/ddc360>
- McCommis KS, Baines CP (2012) The role of VDAC in cell death: friend or foe? *Biochim Biophys Acta* 1818(6):1444–1450. <https://doi.org/10.1016/j.bbamem.2011.10.025>
- Mishra P, Chan DC (2016) Metabolic regulation of mitochondrial dynamics. *J Cell Biol* 212(4):379–387. <https://doi.org/10.1083/jcb.201511036>
- Nagakannan P, Iqbal MA, Yeung A, Thliveris JA, Rastegar M, Ghavami S, Eftekharpour E (2016) Perturbation of redox balance after thioredoxin reductase deficiency interrupts autophagy-lysosomal degradation pathway and enhances cell death in nutritionally stressed SH-SY5Y cells. *Free Radic Biol Med* 101:53–70. <https://doi.org/10.1016/j.freeradbiomed.2016.09.026>
- Neitemeier S, Jelinek A, Laino V, Hoffmann L, Eisenbach I, Eying R, Ganjam GK, Dolga AM, Oppermann S, Culmsee C (2017) BID links ferroptosis to mitochondrial cell death pathways. *Redox Biol* 12:558–570. <https://doi.org/10.1016/j.redox.2017.03.007>
- Olney JW (1969) Brain lesions, obesity, and other disturbances in mice treated with monosodium glutamate. *Science* 164(3880):719–721
- Otera H, Ohsakaya S, Nagaura Z, Ishihara N, Mihara K (2005) Export of mitochondrial AIF in response to proapoptotic stimuli depends on processing at the intermembrane space. *EMBO J* 24(7):1375–1386. <https://doi.org/10.1038/sj.emboj.7600614>
- Pamenter ME, Perkins GA, Gu XQ, Ellisman MH, Haddad GG (2013) DIDS (4,4-diisothiocyanatostilbenedisulphonic acid) induces apoptotic cell death in a hippocampal neuronal cell line and is not neuroprotective against ischemic stress. *PLoS ONE* 8(4):e60804. <https://doi.org/10.1371/journal.pone.0060804>
- Polster BM, Basanez G, Etxebarria A, Hardwick JM, Nicholls DG (2005) Calpain I induces cleavage and release of apoptosis-inducing factor from isolated mitochondria. *J Biol Chem* 280(8):6447–6454. <https://doi.org/10.1074/jbc.M413269200>
- Rambold AS, Kostecky B, Elia N, Lippincott-Schwartz J (2011) Tubular network formation protects mitochondria from autophagosomal degradation during nutrient starvation. *Proc Natl Acad Sci USA* 108(25):10190–10195. <https://doi.org/10.1073/pnas.1107402108>
- Reddy PH (2013) Is the mitochondrial outer membrane protein VDAC1 therapeutic target for Alzheimer's disease? *Biochim Biophys Acta* 1832(1):67–75. <https://doi.org/10.1016/j.bbadis.2012.09.003>
- Sahlender DA, Savtchouk I, Volterra A (2014) What do we know about gliotransmitter release from astrocytes? *Philosophical transactions of the Royal Society of London Series B, Biol Sci* 369(1654):20130592. <https://doi.org/10.1098/rstb.2013.0592>
- Sanderson TH, Raghunayakula S, Kumar R (2015) Release of mitochondrial Opa1 following oxidative stress in HT22 cells. *Mol Cell Neurosci* 64:116–122. <https://doi.org/10.1016/j.mcn.2014.12.007>
- Santello M, Cali C, Bezzi P (2012) Gliotransmission and the tripartite synapse. *Adv Exp Med Biol* 970:307–331. https://doi.org/10.1007/978-3-7091-0932-8_14

- Savtchouk I, Volterra A (2018) Gliotransmission: beyond black-and-white. *J Neurosci* 38(1):14–25. <https://doi.org/10.1523/JNEUROSCI.0017-17.2017>
- Shoshan-Barmatz V, Mizrahi D (2012) VDAC1: from structure to cancer therapy. *Front Oncol* 2:164. <https://doi.org/10.3389/fonc.2012.00164>
- Shoshan-Barmatz V, Zakar M, Rosenthal K, Abu-Hamad S (2009) Key regions of VDAC1 functioning in apoptosis induction and regulation by hexokinase. *Biochim Biophys Acta* 1787(5):421–430. <https://doi.org/10.1016/j.bbabi.2008.11.009>
- Shoshan-Barmatz V, Keinan N, Abu-Hamad S, Tyomkin D, Aram L (2010) Apoptosis is regulated by the VDAC1 N-terminal region and by VDAC oligomerization: release of cytochrome c, AIF and Smac/Diablo. *Biochim Biophys Acta* 1797(6–7):1281–1291. <https://doi.org/10.1016/j.bbabi.2010.03.003>
- Shoshan-Barmatz V, De S, Meir A (2017) The mitochondrial voltage-dependent anion channel 1, Ca(2+) transport, apoptosis, and their regulation. *Front Oncol* 7:60. <https://doi.org/10.3389/fonc.2017.00060>
- Shoshan-Barmatz V, Nahon-Crystal E, Shteinfein-Kuzmine A, Gupta R (2018) VDAC1, mitochondrial dysfunction, and Alzheimer's disease. *Pharmacol Res* 131:87–101. <https://doi.org/10.1016/j.phrs.2018.03.010>
- Su B, Wang X, Zheng L, Perry G, Smith MA, Zhu X (2010) Abnormal mitochondrial dynamics and neurodegenerative diseases. *Biochim Biophys Acta* 1802(1):135–142. <https://doi.org/10.1016/j.bbabi.2009.09.013>
- Tan S, Schubert D, Maher P (2001) Oxytosis: a novel form of programmed cell death. *Curr Top Med Chem* 1(6):497–506
- Twig G, Shirihai OS (2011) The interplay between mitochondrial dynamics and mitophagy. *Antioxid Redox Signal* 14(10):1939–1951. <https://doi.org/10.1089/ars.2010.3779>
- van Leyen K, Siddiq A, Ratan RR, Lo EH (2005) Proteasome inhibition protects HT22 neuronal cells from oxidative glutamate toxicity. *J Neurochem* 92(4):824–830. <https://doi.org/10.1111/j.1471-4159.2004.02915.x>
- Voronina SG, Barrow SL, Gerasimenko OV, Petersen OH, Tepikin AV (2004) Effects of secretagogues and bile acids on mitochondrial membrane potential of pancreatic acinar cells: comparison of different modes of evaluating DeltaPsi_m. *J Biol Chem* 279(26):27327–27338. <https://doi.org/10.1074/jbc.M311698200>
- Zhou Y, Danbolt NC (2014) Glutamate as a neurotransmitter in the healthy brain. *J Neural Transm (Vienna)* 121(8):799–817. <https://doi.org/10.1007/s00702-014-1180-8>